Practical Papers, Articles and Application Notes

Robert G. Olsen, Technical Editor

In this issue you will find two practical papers that should interest members of the EMC community. The first is entitled "Non-conservative Electric Fields, a Demonstration for an Introductory Electromagnetism Course," by A.P.J. van Deursen and H.M. van der Zanden. The authors have developed a very interesting device that can be used to demonstrate magnetically induced (hence non-conservative) electric fields. They have also augmented the experiment with demonstrations that can lead to a better understanding of receiving antennas. These ideas are not always easy to visualize and experiments such as this one are helpful to many of us who want to develop more intuition about electromagnetism. I think that your level of understanding will be increased if you read this article. The second is entitled, "The OATS Method Revisited" by Christopher L. Holloway, Perry Wilson and Robert F. German. I hope that this will be the beginning of a discussion in this Newsletter about the future of radiated emissions measurements and would welcome contributions from others on the subject.

The purpose of this section is to disseminate practical information to the EMC community. In some cases the material is entirely original. In others, the material is not new but has been made either more understandable or accessible to the community. In others, the material has been previously presented at a conference but has been deemed especially worthy of wider dissemination. Readers wishing to share such information with colleagues in the EMC community are encouraged to submit papers or application notes for this section of the Newsletter. See page 3 for my e-mail, FAX and real mail address. While all material will be reviewed prior to acceptance, the criteria are different from those of Transactions papers. Specifically, while it is not necessary that the paper be archival, it is necessary that the paper be useful and of interest to readers of the Newsletter.

Comments from readers concerning these papers are welcome, either as a letter (or e-mail) to the Associate Editor or directly to the authors.

Non-conservative Electric Fields, a Demonstration for an Introductory Electromagnetism Course

A.P.J. van Deursen and H.M. van der Zanden
Group EPS, Technische Universiteit Eindhoven
POB 513
Eindhoven, The Netherlands
a.p.j.v.deursen@tue.nl and h.m.v.d.zanden@tue.nl

In introductory courses on electromagnetism, it often appears to be difficult for students to acquire a good understanding of non-conservative fields. Gravity behaves as a conservative field, and all circuit theory is based on assuming a conservative electric field: the sum of voltages in a loop is set to be zero[1]. So the student's problem with understanding a different concept can be readily imagined. With this in mind, a demonstration experiment has been designed to widen the view of students by actually showing a non-conservative electric field (i.e., one with a "rotation" or a "curl") and introducing the concept step-by-step. The second goal of the demo is to show that this electric field can easily be modified by metal or other boundaries, but that a good conducting metal with a closed current path is required to also modify magnetic fields.

[1] In circuit theory, magnetic induction effects (and hence non-conservative electric fields) are assumed to be localized to within inductors. By doing this, the sum of voltages around a loop (including the voltage across the terminals of an inductor) is zero. In the real world, the magnetic field is distributed over space, and the measured voltages depend on the actual circuit layout including the voltmeter and its leads.

The setup consists of an electrolytic tank driven by a magnetic field; see Fig. 1. Two 40 cm diameter horizontal coils in a

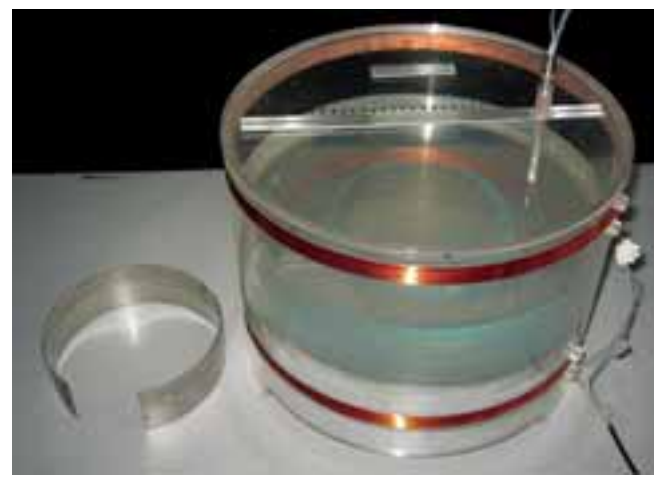

Fig. 1. Photograph of the setup, with the open stainless steel ring at the left.

Helmholtz' configuration produce a vertical magnetic field H_z between them. Each coil has 50 windings. An audio amplifier drives a current through the coils, often at the frequency of about 2 kHz. A horizontal flat plate is glued in the cylindrical coil form to make it a water container. Ten grams of salt is added per liter water to obtain some, but only a small conductivity (σ) of about 0.1 S/m. The water depth is chosen to be 6 cm, and the mid-water-level coincides with the plane midway between the coils where the magnetic field is close to homogeneous. The whole setup is transparent for easy display. For the rest of the presentation it is practical to assume a rectangular (x, y, z) or cylindrical (r, φ, z) coordinate system with a common origin O at the center between the coils, with the axis of symmetry or z-axis vertically.

The magnetic field induces a current in the water, which circulates around the setup axis. Because the water conductivity is relatively small, this current does not significantly reduce the coil's magnetic field. An electric field E_φ is associated with the circulating current density J_φ via Ohm's law $J_\varphi = \sigma E_\varphi$. This E-field can be detected by a sensor, consisting of two small spheres; see Fig. 2. The sensor holder slides in a radial runner in the tank's cover as shown in Fig. 1. The square flange of the holder fixes two perpendicular orientations of the sensor. The length of the wires is chosen such that both spheres move in the mid-water plane, or the plane $z = 0$. A differential amplifier boosts the signal level for display on an oscilloscope. A current probe senses the coil current; its signal is also displayed and serves as a trigger signal for time reference. As is usual in an electrolytic tank, the electric field in the water is approximately equal to the electric field without water. The salted water only serves to provide a sufficiently low impedance between the sensor spheres, such that the cable and the signal amplifier do not load the sensor appreciably. Therefore, the exact value of salt concentration is not critical.

In the first experiment, the sensor slides over a radial path, with the spheres aligned along a circle circumference or the φ-orientation. The sensor signal V_s (a voltage proportional to the electric field between the spheres) appears to be proportional to the radial position to a good approximation, and it changes phase when crossing the z-axis of the setup. The 90 degree phase difference between current and signal is readily seen on the oscilloscope. The signal can be calculated from Faraday's law. Assuming a homogeneous magnetic field H_z, the magnetic flux through a circle of radius r is $\Phi = \mu_0 H_z \pi r^2$. With

$$\oint \vec{E} \cdot \vec{dl} = E_\varphi 2\pi r = -d\Phi/dt = -j\omega\Phi$$

one has $E_\varphi = j\omega\mu_0 H_z r/2$ in common MKSA notation for all quantities. The sensor signal is then $V_s = E_\varphi \ell_s$ with ℓ_s the distance between the sensor spheres, in our case 24 mm. It can

Fig. 2. The sensor holder. The copper wires are insulated and twisted from the spheres up to the twin-lead connector at the top.

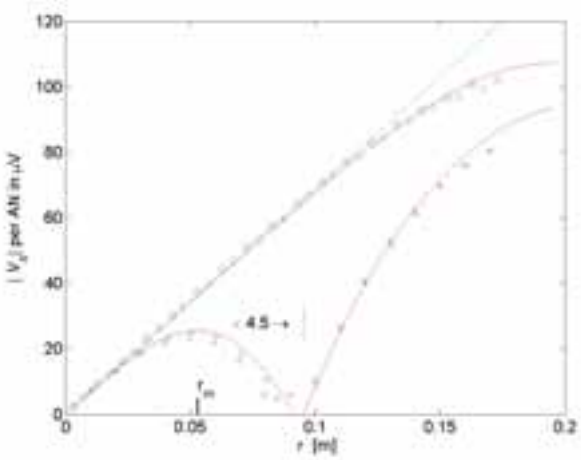

Fig. 3. The sensor signal $|V_s|$ expressed as voltage per ampere-turn (AN) at 2015 Hz, for the setup without a ring (○ and ◇ for both radial sensor positions with respect to the symmetry axis) and with the copper ring (x and +, again for opposite positions). Inside the copper ring, the maximum E_φ or Φ occurs at the radius r_m where $H_z = 0$.

easily be shown that the sensor signal should remain proportional to the radius down to small radii. The measured absolute values are shown in Fig. 3, which includes the data for both radial sensor positions, on opposite sides of the symmetry axis. In this figure, V_s is given as voltage per ampere-winding through the coils, at a frequency of 2015 kHz. The dashed line corresponds to a sensor voltage that would be induced by a homogeneous magnetic field. The solid line takes the actual decrease of the magnetic field into account, which is caused by the non-homogeneity at larger radius. Faraday's law also predicts that the signal is proportional to the frequency. Because of the varying impedance of the coils, a power amplifier that delivers a constant current may be helpful in this part of the demonstration.

The cover can be rotated in the cylindrical part of the setup. At the radius of 0.1 m or larger the signal is quite strong. The sensor voltage is constant in amplitude *and* in phase if one rotates the cover, while keeping the sensor at fixed radial position. So by adding all voltages over a full circle, their sum is definitely not zero, but even large. When the sensor is rotated by 90 degrees around its vertical axis in the runner to align the spheres along the radial direction, the signal drops drastically; in our setup, by a factor of 50 or even better if the angle is adjusted carefully within the limits imposed by the runner in the cover. This demonstrates the φ-orientation of the electric field.

In a second demonstration, a 19 cm diameter copper ring similar to the one shown in Fig. 1, but with the ends connected, is placed around the axis. The copper is 2 mm thick; the ring height is 6 cm. A current is induced in the ring, but because of the high conductivity, the electric field E_φ at the ring is close to zero. This is equivalent to saying that the resistance R of the ring is negligible compared to the reactive impedance ωL. The ring current causes a magnetic field, which opposes the coil field inside the ring. In the $z = 0$ plane where the sensor spheres move, the electric field E_φ is zero on the axis and at the ring, and attains a maximum at some intermediate radius r_m where the total magnetic field H_z is zero. The measured sensor signal is also shown in Fig. 3. Inside the ring, the data are multiplied by a factor of 4.5 for better display. The solid line stems from a simple model for the

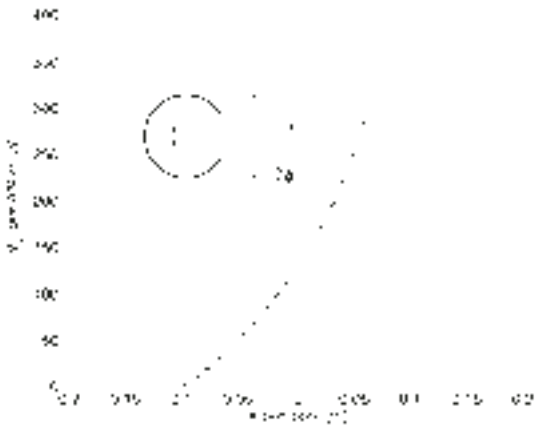

Fig. 4. The sensor signal V_s expressed as voltage per ampere-turn (AN) at 2015 Hz for the open ring.

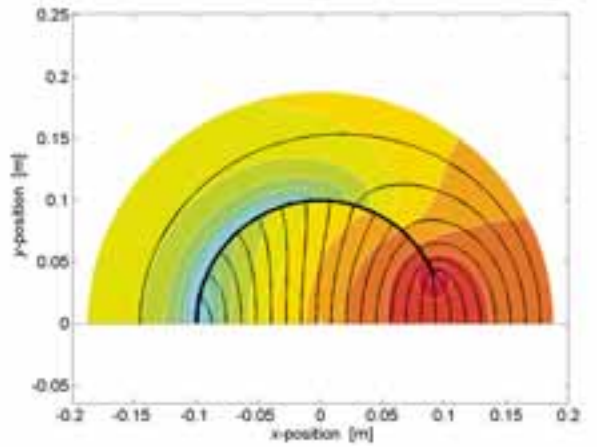

Fig. 5. Electric field lines and magnitude of the field in the setup with the open ring.

current density in the ring. The calculated value of r_m is 5.3 cm.

Because $E_\varphi = 0$ at the ring, the total flux Φ through the ring is also zero. But this does not imply that both magnetic and electric fields inside the ring are small. This would be the case for a very long tube, where a reduction by a factor of 180 would be found for the same copper wall thickness. The current in the ring causes a magnetic flux opposite to the one of the coils. The magnetic field associated with the ring current has to return outside the ring, where it increases the coil field. This explains why V_s rises faster there with the copper ring than without. Still, even at the largest radius V_s remains smaller. Some ring flux returns farther outside. By the same argument, one concludes that the short circuited ring decreases the impedance seen at the coil terminals.

A third demonstration concerns an open stainless steel ring as shown in Fig. 1, mimicking a single turn around a transformer coil. The ring height is again 6 cm, its radius 10 cm. The open angle $2\varphi_0$ is about 45 degrees, as shown in the inset of Fig. 4. This ring breaks the cylinder symmetry, but retains a mirror symmetry with respect to the *x*-axis. The current induced in the metal ring is negligible because it is an open circuit, and so is the E_φ field at the ring surface as can easily be demonstrated by making both sensor spheres touch the ring. The full induced voltage appears over the gap. Accordingly, opposite charges must accumulate at both ring ends in order to increase the electric field between the ends. Figure 4 shows the measured V_s, with the sensor at varying positions over the *x*-axis, and the sensor oriented in the *y*-direction parallel to the electric field there. The ring enhances the electric field in the gap by a factor of 5 on the *x*-axis. Near the ends of the ring the field is even more intense. Smaller gaps would enhance the gap E-field further, since the total induced voltage should remain the same. The solid line in Fig. 4 is calculated with a Method of Moments program; the dashed line stems from a simple two-dimensional charge simulation program.

As Fig. 4 shows, the open ring strongly modifies the electric field. The E-field is oriented perpendicular to the surface. It is instructive to show this behavior with another but smaller sensor. In Fig. 5 we give the result of the charge simulation method over the top half. Thin black lines are the electric field lines; the color shading gives the magnitude of the field on a logarithmic scale. Because the ring current is negligible, the magnetic field is not modified, in contrast to the closed copper ring experiment.

This short paper gives the main ideas of the setup. It is always interesting to see students arriving at the picture of the circular current pattern in the setup without a ring, in spite of the absence of an apparent voltage source. The electric field is distributed, no localized voltage source can be pointed at, and the field changes immediately if any conductor is introduced, even without appreciable current such as the open ring. It usually takes a little more than one hour of class if the demo is presented in a "peer-instruction" way, where students are allowed to discuss each step among them. Other demonstrations are readily imaginable, for instance a predominantly resistive closed stainless steel ring placed either coaxially or off-centered. A full account of the technical details and the modeling will appear in the American Journal of Physics soon. **EMC**

Biographies

A. (Lex) P. J. van Deursen studied Physics at the Radboud Universiteit in Nijmegen, The Netherlands. He also received his PhD degree in Physics at that University in 1976 for an experimental study in Molecular Physics concerning weakly bound atomic and molecular complexes. After a postdoc period at the Max Planck Institut für Festkörperforschung, Hochfeld Magnetlabor in Grenoble (France), he returned to Nijmegen to work in solid state physics on electronic structures of metals, alloys and semiconductors using high magnetic field techniques. In 1986 he moved to Eindhoven University of Technology and shifted his attention to electromagnetic compatibility. He has been engaged in several IEC working groups, and acted as chairman and or member of different committees in international conferences. He is a member of CIGRE SC36.

H (Hennie) M. van der Zanden followed a polytechnical education. He worked in various electronic industries before joining the Eindhoven University in 1979. After different other occupations there, he is now with the group on electrical power systems, where he assists in general pratical teaching and in EMC related research.

The OATS Method Revisited

Christopher L. Holloway and Perry Wilson
National Institute of Standards and Technology
Electromagnetics Division
325 Broadway
Boulder, CO 80305
pfw@boulder.nist.gov and holloway@boulder.nist.gov

Robert F. German
German Training and Consulting, LLC
1410 Moss Rock Place
Boulder, CO 80304
gtc@ieee.org

Abstract:

Open area test sites (OATS) or equivalent semi-anechoic chambers are the most commonly used sites for EMC emissions tests. This article discusses the origins of this test methodology and revisits the interference problem (broadcast media) that the OATS emission test originally addressed. We submit that the interference landscape has changed significantly since the OATS method was developed and that the OATS emission test may not be the best choice to address today's EM environment.

The OATS Method Revisited

In order for manufacturers of digital electronic equipment to market their products worldwide, the products must meet both national and international emissions limits [1],[2]. Products are tested for these unintentional emissions to insure that they will not cause excessive electromagnetic interference (EMI) to radio and television (TV) services. Emission measurements are typically performed using an OATS or an equivalent semi-anechoic chamber. A standard emissions test will find an emissions maximum as a function of both orientation of the equipment under test (EUT) and a scan of the receiving antenna over a 1 m to 4 m height [2],[3]. The emissions maximum is then compared to the appropriate limit to determine whether the EUT passes or fails. While this OATS emission test has served well to limit EMI for many years, it is worthwhile to ask whether it remains the best technical approach in today's electronic environment. To address this question, this article goes back to the roots of the OATS test method and reviews the method's original intent.

Our story begins in the 1960s. During that time, the International Business Machines Corporation (IBM) studied the electromagnetic emissions produced by electronic data processing (EDP) and office machines (OM) [4]. The Computer and Business Equipment Manufacturers Association (CBEMA) later expanded on this work and published a comprehensive report [5]. These studies were conducted with the goals of better understanding interference problems affecting TV and radio reception, and how to develop measurement methodologies, procedures, and field-level emissions limits. The experimental setup for these studies consisted of (a) a TV with a receiving antenna and (b) an EDP or OM device installed in a small building equipped with a raised metal floor. The area between the building and the receive antenna was natural earth. In later years a metallic conducting ground plane was added in order to improve repeatability. The EUT and TV antenna were separated by 30 m and the TV antenna was 10 m above the ground. The choices of a 30 m separation and 10 m antenna height were based on a survey conducted in 12 geographical regions of the United States and Canada. The survey covered 243 EDP installations and 826 antenna locations. The results of the survey showed that 89% of receiving antennas were located at distances of 30 m or more from EDP installations [4],[5]. Thus, the minimal separation of 30 m was chosen in order to maximize interference to the TV antenna. The relative height of VHF/UHF receiving antennas was found to vary between -9 m and 77 m, with 50% of the antennas having a relative height between 7.7 m and 14 m. Thus, a standard height of 10 m was adopted [5]. Field strengths that disrupted TV reception were recorded, and a set of field-strength guidelines was derived.

Over time, various interference problems from other electric devices and products were noted. As a result, the Federal Communications Commission (FCC) concluded that unintentional emissions from digital devices needed to be regulated. The FCC relied on the work of CBEMA [5] for the emissions limits [1]. Hence, the emissions test (i.e., testing a product above a ground plane at a specified antenna separation and height) is based primarily upon interference problems with TV reception. Today, products are tested for either Class A (commercial electronics) or Class B (consumer electronics) limits (see Figure 1): Class A equipment having protection distance of 30 m; Class B equipment having protection distance of 10 m. However, both these test distances can be related to a test performed at a 3 m separation distance [2],[3].

Thus, current emissions test standards are largely based on an interference paradigm (interference to terrestrial broadcast services) that is now much less of a concern. The majority of today's emissions problems are quite different. In a recent report [6], the FCC indicated that 85% of US households receive their TV service from either cable, direct broadcast satellite (DBS), or other multichannel video programming distribution services, and that only 15% of US households receive their TV via direct terrestrial broadcast. Coupling to TV antennas designed to receive terrestrial broadcast may no longer be the most significant interference issue. Different interference scenarios may now be dominant. One example is the proliferation of wireless devices and their potential to cause EMI. Cell phones and pagers are often used in confined spaces (e.g., offices, home, cars, aircraft) containing personal computers (PCs) and other digital devices. The walls, ceiling, floor, and clutter in an office, room, car, or airplane may be highly conductive at high frequencies. Hence, interference from digital devices in these scatter-rich enclosures will be very different from the coupling path measured on an OATS. High-frequency scatter-rich environments are better simulated using a reverberation chamber.

The OATS broadcast-oriented configuration can easily miss an emission problem at frequencies where the EUT is electrically large (physically large compared to the wavelength) and has a complicated emission pattern. For example, emissions directed upward away from the receive antenna can be missed. Although such emissions do not cause an EDP and OM device to interfere with a TV connected to a roof-top antenna, they could easily cause a cell phone in a wood-frame building to interfere with a PC

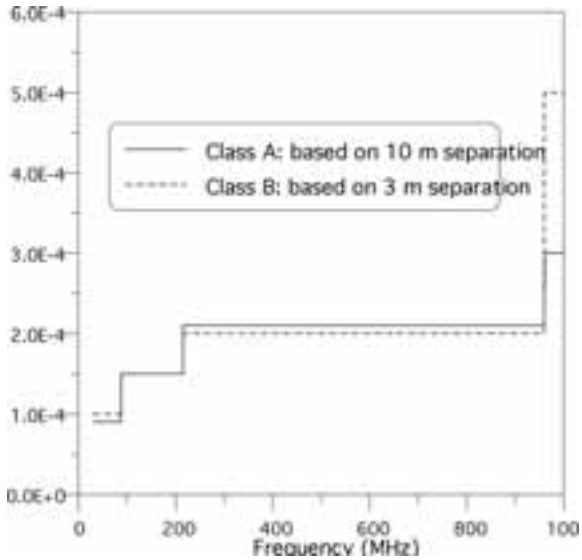

Figure 1: Maximum E-field limit.

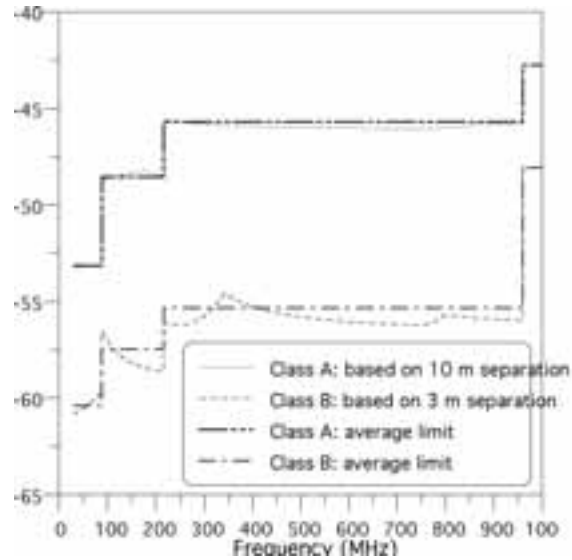

Figure 2: Total radiated power limits.

located on the floor above it. OATS are also subject to ambients. These problems can lead to poor results (missed emissions), either unintentionally or intentionally. In principle, products could be set up for emission measurements in such a manner as to insure that significant emission problems would not be detected using the OATS configuration. And, in principle, ambients could be used to mask emissions. To avoid these pitfalls, alternatives to the OATS need to be considered and possibly be made the reference site for emissions measurements that do not primarily target the protection of broadcast receivers.

The two primary alternatives mentioned above are reverberation chambers and fully-anechoic chambers. Reverberation chambers will detect emissions in all directions and at all frequencies; however, reverberation chambers negate gain. Fully-anechoic chambers will detect emissions at all frequencies; however, the test object needs to be rotated if all directions are to be checked. Thus, if reverberation chambers and fully-anechoic chambers are to be used, then new emission limits and test methodologies will be needed [7]. Ideally, these new limits should be based on the type of product functionality we are protecting. This requires comprehensive field studies similar to the ones used to develop the OATS limits. Once such comprehensive studies are available, a reverberation chamber emission standard could be based on the total radiated power, as measured in the chamber, and a representative directivity that when combined give new and more appropriate field limits. An example of total radiated power limits for reverberation chambers that are approximately equivalent to the current OATS standard are shown in Figure 2, see [7] for detail.

For the near term, the OATS type of emissions measurement will remain the method by which most electric products are tested. Although this methodology is still appropriate to minimize interference between a digital device installed on a raised metal floor and a TV connected to a roof-top antenna, the evolution of digital devices will continue to change the EMI landscape. Test methods that more closely replicate a high frequency scatter-rich environment or a low-frequency free-space environment will inevitably become preferable. Thus, it may be time to test the new generation of small computing devices in a reverberation chamber or a fully-anechoic chamber and (with tongue firmly in cheek) save OATS for the breakfast table and the cookie platter.

References

[1] Code of Federal Regulations, Title 47: Telecommunication, Part 15: Radio Frequency Devices, Section 15.109: Radiated Emission Limits. Office of the Federal Register, National Archives and Records Administration, Oct. 1, 2004.

[2] CISPR 22-2003, "Information Technology Equipment - Radio Disturbance Characteristics - Limits and Methods of Measurement", International Electrotechnical Commission, Fourth Edition, April 2003.

[3] ANSI C63.4-2003, "Methods of Measurement of Radio - Noise Emissions from Low-Voltage Electrical and Electronic Equipment in the Range 9 kHz to 40 GHz", American National Standards Institute, 2003.

[4] R.E. Boyd, J.A. Malack, and I.E. Rosenbarker, "EMI control for data processing and office equipment," in Proc. of Electromagnetic Compatibility 1975: 1st Symposium and Technical Exhibition on Electromagnetic Compatibility, Montreux, Switzerland, May 20-22, 1975, pp. 307-313.

[5] "Limits and methods of measurement of electromagnetic emanations from electronic data processing and office equipment," Computer and Business Equipment Manufacturers Association (CBEMA) Environment and Safety (ESC), subcommittee SC5 on Electromagnetic Interference, Report CBEMA/ESC5'77'29, Washington, DC, May 20, 1977.

[6] Annual assessment of the status of competition in the market for the delivery of video programming. Seventh Annual Report, Federal Communications Commission, CS Docket No. 00-132; Jan. 8, 2001.

[7] C.L. Holloway, P.F. Wilson, G. Koepke and M. Candidi, "Total Radiated Power Limits for Emission Measurements in a Reverberation Chamber," Proc. 2003 IEEE International Symposium on Electromagnetic Compatibility, Boston, MA, August, 2003.

Mention of any company names serves only for identification, and does not constitute or imply endorsement of such a company or of its products.

Biographies

Christopher L. Holloway (S'86-M'92-SM'04) received the Ph.D. degree in electrical engineering from the University of Colorado in 1992. He is currently with the National Institute of Standards and Technology in Boulder, CO after previous positions with Electro Magnetic Applications, the National Center for Atmospheric Research (NCAR), and the Institute for Telecommunications Sciences (ITS). His research interests include electromagnetic field theory, wave propagation, guided wave structures, remote sensing, numerical methods, and EMC/EMI.

Perry F. Wilson (S'78-M'82-SM'93-F'05) received his Ph.D. in Electrical Engineering from the University of Colorado in 1983. He is presently with the National Institute of Standards and Technology in Boulder, CO after previous positions with Asea Brown Boveri (ABB) and the Institute for Telecommunication Sciences (ITS). His interests include electromagnetic theory as applied to EMC problems, radio frequency field metrology, and wireless communications.

Robert F. German is the manager of German Training and Consulting, LLC, in Boulder, CO. He consults on the EMC design of digital devices and EMC test facilities. Mr. German is a NARTE certified EMC engineer and a Senior Member of the IEEE. He received the MSEE degree from the University of Colorado, Boulder, CO in 1979, the BSEE degree from the University of Miami, Coral Gables, FL in 1974, and was born in Bridgeport, CT in 1952. Mr. German can be contacted at 303-444-2472 or gtc@ieee.org.